Available online at www.sciencedirect.com
ScienceDirect
Biomaterials 28 (2007) 256–270
Biomaterials
www.elsevier.com/locate/biomaterials

Assessment of hepatocellular function within PEG hydrogels

Gregory H. Underhill[a,1], Alice A. Chen[a,1], Dirk R. Albrecht[a], Sangeeta N. Bhatia[a,b,*]

[a]*Harvard—M.I.T. Division of Health Sciences and Technology/Electrical Engineering and Computer Science, Massachusetts Institute of Technology, 77 Massachusetts Ave., E19-502D, Cambridge, MA, USA*
[b]*Division of Medicine, Brigham and Women's Hospital, Boston, MA, USA*

Received 18 April 2006; accepted 23 August 2006
Available online 18 September 2006

Abstract

Tissue-engineered therapies for liver failure offer the potential to augment or replace whole organ transplantation; however, fabrication of hepatic tissue poses unique challenges largely stemming from the complexity of liver structure and function. In this study, we illustrate the utility of highly-tunable, photopolymerizable poly(ethylene glycol) (PEG) hydrogels for 3D encapsulation of hepatic cells and highlight a range of techniques important for examining hepatocellular function in this platform. Owing to our long-term interest in incorporating proliferative progenitor cell types (e.g. hepatoblasts, oval cells, or cells derived from embryonic stem cells) and maintaining the phenotype of differentiated cells, we explored the behavior of bipotential mouse embryonic liver (BMEL) cells as a model progenitor cell and mature, fully differentiated, primary hepatocytes in this biomaterial system. We demonstrated the importance of cell–cell and cell–matrix interactions in the survival and function of these cell types, and the capacity to influence encapsulated cell phenotypes through modulation of hydrogel characteristics or gene silencing. Additionally, we demonstrated imaging techniques critical for the in situ assessment of encapsulated hepatocyte function combined with the ability to control cellular organization and overall architecture through microscale patterning technologies. Further analysis of liver progenitor as well as mature hepatocyte processes within the versatile PEG hydrogel platform will aid in the development of tissue engineered implantable liver systems.

Keywords: Hydrogel; Hepatocyte; Progenitor cell; Liver

1. Introduction

Due to the complexity of liver function, it has been proposed that development of cell-based therapies will be necessary to provide alternatives to whole organ transplantation for liver failure [1]. Cell-based strategies include temporary support systems such as extracorporeal devices that typically house hepatocytes or hepatocyte-derived cell lines to process patient plasma or implantable 'tissue engineered' constructs [1,2]. Development of implantable constructs is a complex challenge constrained by the high metabolic rate of the liver [3], the need for unimpeded transport for large macromolecules, and the complex architecture required for the interaction of multiple cell types—minimally, hepatocytes and cholangiocytes. In addition, interfacing primary hepatocytes with biomaterials is challenging as their phenotype is unstable under many conditions, they are adhesion-dependent, relatively immotile, and do not proliferate substantially ex vivo [1]. As a result, various hepatic tissue engineering approaches have been explored including the attachment of hepatocytes to microcarriers [4,5], implantation of ex vivo cultured liver organoids or encapsulated hepatocyte spheroids [6–8], as well as the immobilization of hepatic cells on or within synthetic or biologic scaffolds [9–11]. These techniques have shown some limited success; however, very few platforms allow control over both scaffold chemistry and architecture-features which can independently influence hepatocyte survival and function. Due to its versatility, we sought to develop a poly(ethylene glycol) (PEG)-based hydrogel system as a platform for hepatic tissue engineering. These photopolymerizable

*Corresponding author. Harvard—M.I.T. Division of Health Sciences and Technology/Electrical Engineering and Computer Science, Massachusetts Institute of Technology, 77 Massachusetts Avenue, E19-502D, Cambridge, MA, USA. Tel.: +1 617 324 0221; fax: +1 617 324 0740.
E-mail address: sbhatia@mit.edu (S.N. Bhatia).
[1]Gregory H. Underhill and Alice A. Chen contributed equally.

0142-9612/$ - see front matter © 2006 Elsevier Ltd. All rights reserved.
doi:10.1016/j.biomaterials.2006.08.043

materials have been increasingly utilized in tissue engineering applications due to their hydrophilicity and resistance to protein adsorption, biocompatibility, and the ability to customize such gels through the modification of chain length and the addition of degradable linkages, adhesive peptides, and other biologically active factors [12,13]. PEG-based hydrogels have been used for the encapsulation of a diverse array of cell types in a 3D context including chondrocytes [14–19], fibroblasts [20–23], vascular smooth muscle cells [24,25], osteoblasts [26,27], neural precursor cells [28], and mesenchymal stem cells [29–33]. Analogous to these other systems, tissue engineering of hepatocellular constructs is a promising cell-based therapy for liver disease, and additionally can serve as an important platform for in vitro analysis of cell fate and function within a 3D microenvironment.

Even with the development of the appropriate biomaterial platform, lack of hepatocyte proliferation is likely to limit the success of hepatic tissue engineering approaches. Therefore, we are interested in developing platforms that could incorporate both proliferative hepatic progenitors and mature, differentiated cell types. In particular, fetal hepatoblasts are an intriguing potential cell type for liver cell-based therapies. Hepatic development proceeds through the differentiation of hepatoblasts that display bipotential differentiation capacity, which is defined by the ability to differentiate into both hepatocytes and cholangiocytes [34]. Recent work by Strick-Marchand et al. [35,36] demonstrates the development of bipotential mouse embryonic liver (BMEL) cell lines that are derived from mouse E14 embryos. These cell lines are nontransformed and exhibit bipotential differentiation in vivo as well as under specific culture conditions in vitro. Taken together, the inducible differentiation of BMEL cells in culture and the appropriate bipotential differentiation of these cells within distinct microdomains of the liver suggests that microenvironmental stimuli are likely important in regulating BMEL cell fate and function. Consequently, examination of BMEL cells within biomaterial platforms, such as adaptable synthetic PEG-based hydrogel networks, could potentially represent a robust approach for examining the impact of extracellular stimuli and cellular organization on BMEL cell responses. Furthermore, despite their inducible differentiation in vitro and their ability to migrate to the liver and participate in liver regeneration, the potential utility of BMEL cells for tissue engineered implantable constructs remains unexplored.

In this study, we sought to examine the utility of PEG hydrogels as a platform for hepatic tissue engineering. Specifically, we aimed to establish experimental conditions to promote viability and function of both BMEL cells and hepatocytes. We hypothesized that microenvironmental factors such as the degree of cell–cell interactions, the presence of adhesive sequences, and hydrogel parameters such as PEG chain length would influence hepatocellular function within the framework of the 3D hydrogel. In addition, in order to enhance the effectiveness of these systems for both in vitro analysis and implantable therapeutic constructs, we also aimed to develop methods to fabricate replicate samples in parallel, examine structure/function relationships in a 3D context, and probe molecular mechanisms of interest using RNA interference. Collectively, the examination of hepatocellular function within PEG hydrogels requires a distinct set of cellular and molecular biology techniques. Here, we highlight several techniques important for the analysis of BMEL cell and primary hepatocyte viability and function upon encapsulation within PEG hydrogel networks. In particular, for the BMEL cells, these include assays for encapsulated cell viability, for which we show improvement due to augmented cell–cell interactions. Moreover, we demonstrate gene expression analysis within the hydrogel platform, including alterations indicative of differentiation as well as siRNA-mediated gene silencing. For primary hepatocytes, we illustrate assays important for the assessment of encapsulated hepatocyte function, such as urea synthesis and albumin secretion, and the influence of PEG chain length and weight percentage on albumin release. Additionally, we report the increased maintenance of primary hepatocyte function within PEG hydrogels due to co-culture with fibroblasts and the addition of the adhesive peptide, RGDS. We also show in situ measures of encapsulated hepatocyte function, such as intracellular albumin production and glycogen storage, important for determining cellular localization and spatial distribution of functions within the hydrogel. Finally, we utilize photopatterning to generate an array of BMEL cell hydrogel constructs and photopatterning and dielectrophoretic patterning techniques to build hepatocyte/fibroblast co-culture networks with defined organization.

2. Materials and methods

2.1. Cell culture

The BMEL cell line, 9A1, was provided by Dr. Mary Weiss (Institut Pasteur) and cultured as described previously [35,36]. In brief, cells were maintained in collagen coated flasks in RPMI 1640 medium with glutamax (Invitrogen), containing 30 ng/mL human IGF-II (Peprotech), 50 ng/mL human EGF (Peprotech), and 10 μg/mL recombinant human insulin (Invitrogen) and passaged every 2–4 days. BMEL cell aggregates were formed by culturing 5×10^6 cells in 100 mm non-adhesive suspension dishes. For hydrogel experiments, BMEL cells were cultured in non-adhesive dishes for 7–24 h to form aggregates prior to encapsulation.

Hepatocytes from 2- to 3-month-old adult female Lewis rats (Charles River Laboratories) were isolated and purified as previously described [37,38] and cultured at 37 °C, 5% CO_2 in hepatocyte medium consisting of DMEM with high glucose (Invitrogen), 10% fetal bovine serum (FBS, Invitrogen), 0.5 U/mL insulin (Lilly), 7 ng/mL glucagons (Bedford Laboratories), 7.5 μg/mL hydrocortisone (Sigma), 10 U/mL penicillin (Invitrogen), and 10 μg/mL streptomycin (Invitrogen). 3T3-J2 fibroblasts were provided by Howard Green (Harvard Medical School, Cambridge, MA) [39] and cultured at 37 °C, 5% CO_2 in fibroblast medium consisting of Dulbecco's modified eagle medium (DMEM) with high glucose, 10% FBS, and 1% penicillin-streptomycin. Fibroblasts were passaged no more than 14 times.

Conditions for hepatocyte-fibroblast co-culture have been described previously [40,41]. Briefly, freshly isolated hepatocytes were seeded at a

density of 5.0×10^5 cells per well in 34-mm wells adsorbed with 0.13 mg/mL Collagen-1 extracted from rat-tail tendons [38]. Twenty-four hours after seeding hepatocytes, 5.0×10^5 fibroblasts were seeded in fibroblast medium. Fibroblast medium was replaced with hepatocyte medium 24 h later and subsequently exchanged daily for 7–10 days, at which time hepatocyte-fibroblast co-cultures were harvested for hydrogel encapsulation.

2.2. Hydrogel materials

PEG diacrylate (PEG-DA) of molecular weight 3.4 and 20 kDa was obtained from Nektar Therapeutics (Huntsville, AL). To prepare PEG monoacrylate conjugated peptides, RGDS or RGES peptides (American Peptide, Sunnyvale, CA) were dissolved in 50 mM sodium bicarbonate (pH 8.5) at 4 mg/mL. Acrylate-PEG-NHS (3.4 kDa, Nektar) was added at a 1:1 molar ratio and reacted at room temperature for 2.5 h. The reaction mixture was subsequently dialyzed (MWCO 2 kDa), lyophilized, and stored at −20 °C under nitrogen.

2.3. Hydrogel encapsulation of BMEL cells and primary hepatocytes

For hydrogel encapsulation of BMEL cells, dispersed or aggregated cells were resuspended at a 2X final concentration in BMEL cell culture medium following a 2 h treatment with 100 μg/mL ascorbic acid (Sigma). The cell suspension was then added 1:1 to a 3.4 kDa PEG-DA pre-polymer solution in PBS (Gibco). The final concentrations of components were 10×10^6 BMEL cells/mL, 10% w/v 3.4 kDa PEG-DA, and 0.05% w/v Irgacure 2959 photoinitiator (I-2959, Ciba). For all experiments excluding patterning experiments, 250 μm thick, 1.1 cm diameter hydrogels were prepared on 18 mm cover glass circles (Fisher Scientific) by exposure to 320–390 nm UV light (10 mW/cm^2) for 70 s, using a polymerization apparatus previously described in detail [42]. The light source utilized was an EXFO Lite UV spot curing system equipped with a collimating lens (EXFO, Mississuaga, ON, Canada). Hydrogels were subsequently washed with PBS, followed by culture medium, and then cultured in BMEL cell culture medium with media changes every other day.

For primary hepatocyte encapsulation, excluding patterning experiments, 250 μm thick, 1.1 cm diameter hydrogels were formed by exposure to 320–390 nm UV light (10 mW/cm^2) for 50–60 s with 0.1% w/v I-2959. Both 10% w/v 3.4 kDa PEG-DA and 10% w/v 20 kDa PEG-DA were prepared as indicated. Unless otherwise noted, hepatocytes and hepatocyte/fibroblast co-culture cells were encapsulated at a density of 7.5×10^6 hepatocytes per milliliter of pre-polymer solution. For co-culture gels utilized for functional experiments, hepatocytes and fibroblasts coordinately removed from 2D co-cultures were encapsulated together in bulk. For peptide experiments, acrylate-PEG-RGDS or acrylate-PEG-RGES was added to the pre-polymer formulation at 20 μmol/mL. Hepatocyte-containing hydrogels were cultured in hepatocyte medium, which was changed daily.

2.4. Assessment of encapsulated cell viability

Cell viability was examined utilizing labeling with calcein AM (5 μg/mL) and ethidium homodimer (2.5 μg/mL) (live/dead) fluorescent stains (Molecular Probes). Viable and nonviable cells were manually counted for four regions on replicate gels and the mean percentage of viable cells was determined. Images were acquired using a Nikon Ellipse TE200 inverted fluorescence microscope and CoolSnap-HQ Digital CCD Camera. Viability of encapsulated cells was additionally quantified using the dimethylthiazol-diphenyltetrazolium bromide (MTT) assay. Duplicate hydrogels for each condition were incubated in phenol red-free DMEM (Gibco) containing 0.5 mg/mL MTT (Sigma) for 1 h at 37 °C. The resulting precipitate was then solubilized by the addition of 50% isopropanol/50% DMSO and the absorbance at 570 nm (minus background absorbance at 660 nm) was quantified. Absorbance measures were normalized to day 0 values and the mean and standard deviation of three independent experiments was calculated, with statistical significance determined using a Student's *t*-test.

2.5. Gene expression analysis and short interfering RNA transfection

To examine gene expression of hydrogel encapsulated BMEL cells, 4–6 hydrogels of each condition were pestle homogenized in Trizol (Invitrogen) and total RNA was isolated according to the manufacturer's instructions. Subsequently, total RNA was incubated with RNase-free DNase (New England Biolabs) at 37 °C for 40–60 min and further cleaned using RNeasy spin columns (Qiagen). For adherent BMEL cells or suspension BMEL aggregates, approximately 0.5×10^6 cells were pelleted and resuspended in the Trizol reagent. 0.5 μg of total RNA was used in 20 μL cDNA synthesis reactions utilizing the iScript™ cDNA synthesis kit (Bio-Rad, Hercules, CA) according to the manufacturer's protocol, and reactions performed in the absence of reverse-transcriptase enzyme were used as negative controls. cDNA products then served as templates in 25 μL PCR reactions with the iQ™ SYBR green supermix (Bio-Rad) and reactions were performed and analyzed using the MyiQ™ real-time PCR detection system (Bio-Rad). The cycling parameters were 95 °C for 3 min then 40 cycles of 95 °C for 10 s and 60 °C for 45 s. Primers for albumin, ADH, lamin A, and the housekeeping gene, HPRT, were used at 100 nM and were purchased from Integrated DNA Technologies (Coralville, IA). Primer sequences are available upon request. HPRT mRNA expression was utilized as a normalization control, and the mean expression of albumin and ADH by encapsulated BMEL aggregates from three independent experiments is displayed relative to the basal expression exhibited by adherent BMEL cells prior to aggregation.

Fluorescently labeled lamin A (NM_019390) siRNA bearing a fluorescein molecule on the 5′ end of the sense strand was designed and purchased from Dharmacon. The annealed sequence was reconstituted in nuclease-free water. Cell transfection was performed using 100 nM siRNA and Lipofectamine 2000 (Invitrogen) according to manufacturer's instructions. BMEL cells were transfected in collagen coated 100 mm culture dishes, and following a 6 h incubation in BMEL cell culture medium, were transferred to non-adhesive dishes for aggregate formation. After overnight incubation, BMEL cell aggregates were encapsulated in PEG hydrogels or maintained in suspension, and following an additional 24 h culture, four hydrogel samples for each condition were pooled and processed for RNA extraction and gene expression analysis.

2.6. Assessment of hepatocellular function and albumin release

Daily medium samples from encapsulated cell cultures were collected and stored at −20 °C until assayed. Albumin content in spent media samples was quantified using an enzyme-linked immunosorbent assay (ELISA) with horseradish peroxidase detection and peroxidase substrate 3,3′,5,5′-tetramethylbenzidine. Albumin ELISA was also utilized to determine cumulative release of purified albumin from distinct hydrogel configurations. Forty microgram of albumin was encapsulated within 10% 3.4 kDa and 10%, 15%, and 20% 20 kDa PEG hydrogels as described above for hepatocyte-containing hydrogels, and albumin concentration within the hydrogel supernatant was measured at the indicated time points. Urea concentration was quantified using a colorimetric endpoint assay based on acid- and heat-catalyzed condensation of urea with diacetylmonoxime (Stanbio Labs). Error bars represent standard deviation of the mean ($n = 3$), and statistical significance was determined for $p < 0.05$ using one-way ANOVA (analysis of variance) with Tukey post-hoc test.

2.7. Hydrogel sectioning and staining

To demonstrate immunodetection of albumin in encapsulated cells, hydrogels were sectioned using a modified paraffin-processing and

sectioning procedure. Following encapsulation of hepatocyte-fibroblast co-cultures in 10% 20 kDa PEG + RGDS hydrogels, gels were washed twice in cold PBS, fixed in 4% paraformaldehyde at room temperature for 40 min, washed again, dehydrated in increasing gradients of EtOH and embedded in paraffin. Paraffin blocks were sectioned to 10 μm thicknesses. The sections were transferred dry to glass dishes and deparaffinized in solution using three 5-min changes of 100% xylene, three 3-min changes of 100% EtOH, one 3-min change each of 95% EtOH and 70% EtOH and two 3-min changes of distilled deionized H_2O. In solution, the deparaffinized cell-hydrogel sections were permeabilized for 30 min at room temperature in 0.1% Triton-X, washed three times for 10 min each in PBS, blocked for 4 h at 37 °C in 20% goat serum and incubated with primary and secondary antibodies. Primary antibody was rabbit anti-rat albumin (MP Biomedicals, Inc.) diluted 1:100 in 1% bovine serum albumin (1% BSA) and incubated at 4 °C overnight with gentle shaking. Secondary antibody was goat anti-rabbit IgG-FITC (Santa Cruz Biotechnology) diluted 1:100 in 1% BSA and incubated 3 h at 37 °C. Three 30-min PBS washes took place between antibody incubations. Finally, cell-hydrogel sections were washed in PBS, incubated 10 min in 0.005% Hoescht 33342 (Molecular Probes), washed briefly and wet-mounted onto glass slides using Vectashield anti-fade medium (Vector Laboratories) and a glass coverslip. Visualization was performed using phase contrast and epifluorescence microscopy.

Glycogen staining of intact 10% 3.4 kDa hydrogel networks was performed with a modified periodic acid-Schiff (PAS) staining protocol using the commercially available PAS staining kit from Sigma. In brief, duplicate hydrogels were fixed with 3.7% formaldehyde (in 95% ethanol) for 1 min at room temperature followed by two washes with dH_2O. Gels were then incubated in 1% periodic acid for 2 min at room temperature and then washed three times with dH_2O prior to addition of Schiff's reagent. Bright field or Hoffman modulation contrast images were acquired in the presence of the Schiff's reagent and color rendered with Metamorph Image Analysis software.

2.8. Patterning of hydrogel constructs

Photopatterning of hydrogel constructs was achieved using the previously described polymerization apparatus [42]. Clean 18 mm cover glass circles served as platforms for hydrogel polymerization and were treated with a 2% v/v solution of 3-(trimethoxysilyl) propyl methacrylate (Aldrich, Milwaukee, WI) in 95% ethanol (pH 5 with acetic acid) for two minutes, rinsed with 95% ethanol, and then baked at 100 °C for at least 5 min to create free methacrylate groups on the glass. Replicate arrays of cylindrical 500 μm thick hydrogel domains (10% 3.4 kDa PEG-DA), containing 10×10^6 BMEL cells or hepatocytes were polymerized as described above for these cells types, with the UV exposure of the pre-polymer solution localized by the presence of an emulsion mask overlay (diagrammed in Fig. 6). Masks were designed using Corel Draw 11.0 and printed using a commercial Linotronic-Hercules 3300 dpi high-resolution line printer. Arrays with approximately 500 μm regions with 1.3 mm center-to-center spacing and approximately 1 mm regions with 2.5 mm center-to-center spacing were generated for BMEL cell and hepatocyte experiments where indicated. 500 μm and 1 mm regions required 100 and 70 s of UV exposure (10 mW/cm^2), respectively. The subsequent addition of encapsulated fibroblasts, also diagrammed in Fig. 6, in the intermediate regions was achieved by the secondary polymerization (10 mW/cm^2, 50 s) through a blank transparency of a 10% 3.4 kDa PEG-DA solution (0.1% I-2959) containing 10×10^6/mL fibroblasts. Further control of cellular organization within these patterned regions was accomplished through a dielectrophoretic patterning method recently described in detail [43,44]. Briefly, hepatocyte and fibroblast positioning within 100 μm thick hydrogels was controlled utilizing negative dielectrophoresis. During patterning cells were energized with a 2.5 V (rms), 10 kHz a.c. bias for 3 min on a hexagonal electrode array with 100 μm spacing. For these experiments, the pre-polymer suspension was prepared in low-conductivity electropatterning buffer, with 15% w/v 3.4 kDa PEGDA, 0.03% w/v I-2959, and approximately 10×10^6/mL hepatocytes and 12×10^6/mL 3T3 fibroblasts. For photopatterned and dielectrophoretic patterned constructs, live/dead analysis and glycogen staining were performed as described above within 1 h of gel polymerization.

3. Results

3.1. Survival of PEG hydrogel encapsulated BMEL cells

In order to examine the compatibility of BMEL cells with 3D hydrogel culture, we initially encapsulated a monodispersed population of cells within PEG hydrogels utilizing photopolymerization parameters recognized to induce minimal toxicity [45]. As expected, viability, measured by calcein AM/ethidium homodimer (live/dead) labeling, was high (95.3 ± 0.4%) within 1 h of encapsulation (Fig. 1A). However, the viability of dispersed BMEL cells in hydrogel culture decreased rapidly to, on average, only 24.7 ± 0.3% by 3 days post-encapsulation (Fig. 1B). On the contrary, BMEL cells pre-aggregated for 24 h into spheroids did not exhibit this marked decrease in cell viability (Figs. 1C and D). This effect of aggregation on BMEL cell survival in PEG hydrogels was also independently verified utilizing the MTT assay, a quantitative measure of cellular metabolism. In particular, pre-aggregated BMEL cells showed a significant increase in viability versus dispersed cells at 1, 2, and 3 days post-encapsulation (Fig. 1E). Viability measured using the MTT assay correlated with the fluorescent labeling data, with dispersed BMEL cells at day 3 exhibiting a 77.1% decrease in viability relative to day 0. These results demonstrate a key role for cell–cell interactions in the maintenance of BMEL viability within PEG hydrogels, and correlate with the documented importance of aggregate culture in the regulation of BMEL differentiation.

3.2. Gene expression analysis of encapsulated BMEL aggregates

The formation of BMEL cell aggregates in suspension culture has been previously demonstrated to induce the acquisition of hepatocyte phenotypes [35]. In order to determine if BMEL cells encapsulated within PEG hydrogels are capable of upregulating hepatocyte markers, total RNA was isolated from encapsulated BMEL aggregates and the expression of transcripts encoding albumin and alcohol dehydrogenase (ADH) was assessed using quantitative RT-PCR. Indeed, encapsulated BMEL aggregates displayed a substantial induction of both albumin and ADH, with an average induction at 5 days post-encapsulation of 210-fold and 41,740-fold, respectively, each determined relative to basal levels exhibited by adherent cells (Fig. 2A). Interestingly, albumin and ADH expression demonstrated somewhat different kinetics, with albumin mRNA levels increasing an average of 3.2-fold from day 1 to day 5, whereas ADH mRNA expression increased an additional 37.5-fold in this time period (Fig. 2A). Overall, the induction of albumin and ADH, both important

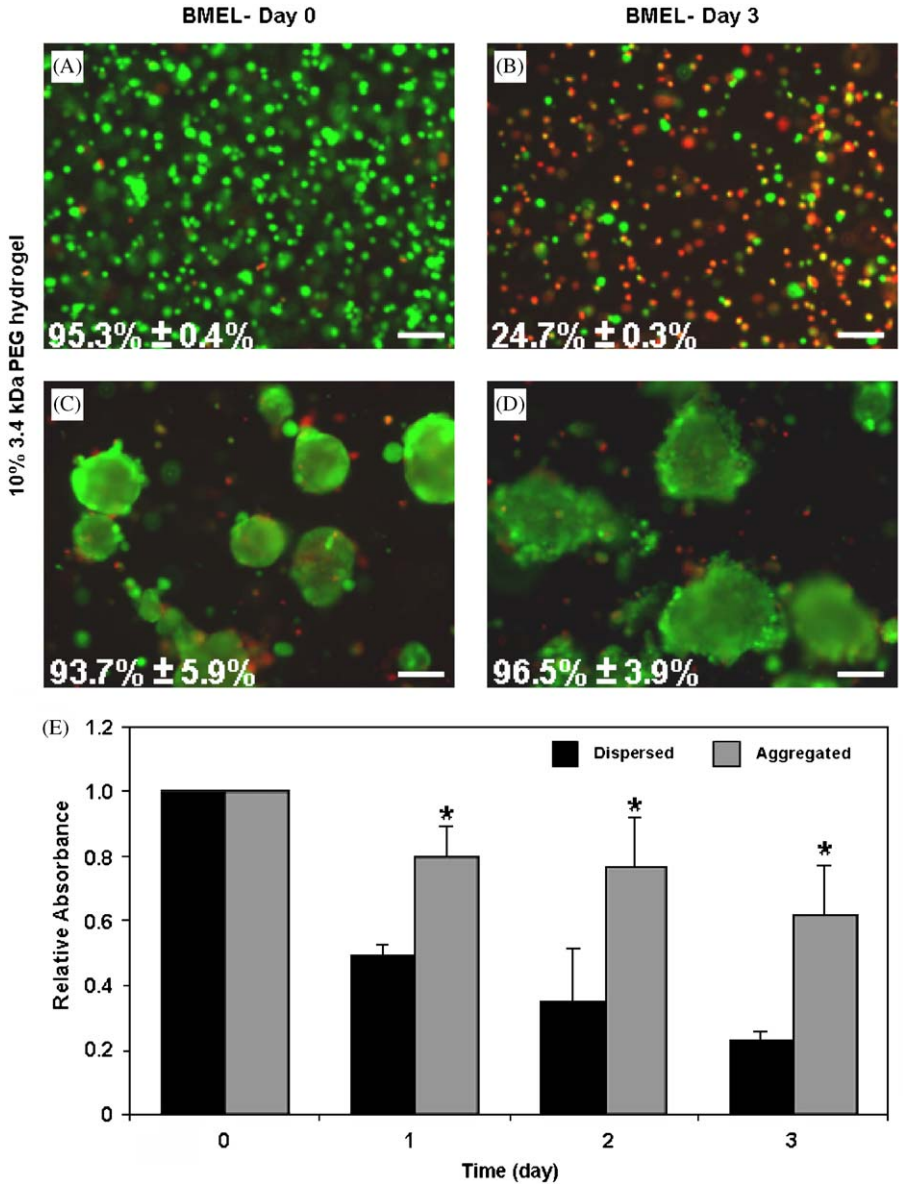

Fig. 1. Aggregation improves survival of BMEL cells in PEG hydrogel culture. (A, B) Viability of dispersed BMEL cells encapsulated in 10% 3.4 kDa PEG hydrogels was evaluated on days 0 and 3. Fluorescent labeling distinguished viable (green) from nonviable (red) cells. The percentage of viable cells (mean ± SD, $n = 4$) at each time point is indicated. (C, D) Viability labeling was similarly performed for encapsulated BMEL cell aggregates on day 0 and day 3 of hydrogel culture. Scale bars (A–D): 100 μm. (E) Survival of dispersed BMEL cells (black bars) and BMEL cell aggregates (grey bars) at multiple time points following encapsulation was quantitatively compared using the MTT assay. Absorbance measures are normalized to day 0 values. Data are mean ± SD ($n = 3$, independent experiments). The (*) indicates statistical significance relative to dispersed cells at the respective time points, $p < 0.05$ (Student's t-test).

markers of hepatocyte differentiation, exhibited by encapsulated cells illustrates that BMEL cell differentiation can occur within the PEG hydrogel platform.

The ability to manipulate BMEL cell gene expression within PEG hydrogels through technologies such as RNA interference would represent an important tool for understanding BMEL cell differentiation and function within a 3D model system. Consequently, in order to demonstrate the efficacy of siRNA-mediated gene knockdown for hydrogel encapsulated BMEL cells, we examined silencing efficiency for a representative target gene, the gene encoding the nuclear lamin protein, lamin A (LMNA). Transfection of BMEL cells with fluorescein-labeled LMNA siRNA prior to aggregation and encapsulation enabled the visualization of transfected cells within the PEG hydrogels (Fig. 2B, inset). Quantitative RT-PCR analysis demonstrated a significant reduction in LMNA gene expression for hydrogel encapsulated BMEL aggregates at 2 days post-transfection (Fig. 2B). Furthermore, this reduction was similar to the amount observed for non-encapsulated aggregates in suspension (Fig. 2B), suggesting that hydrogel encapsulation does not directly affect the maintenance of gene knockdown. Taken together, these results highlight the capacity to quantitatively assess

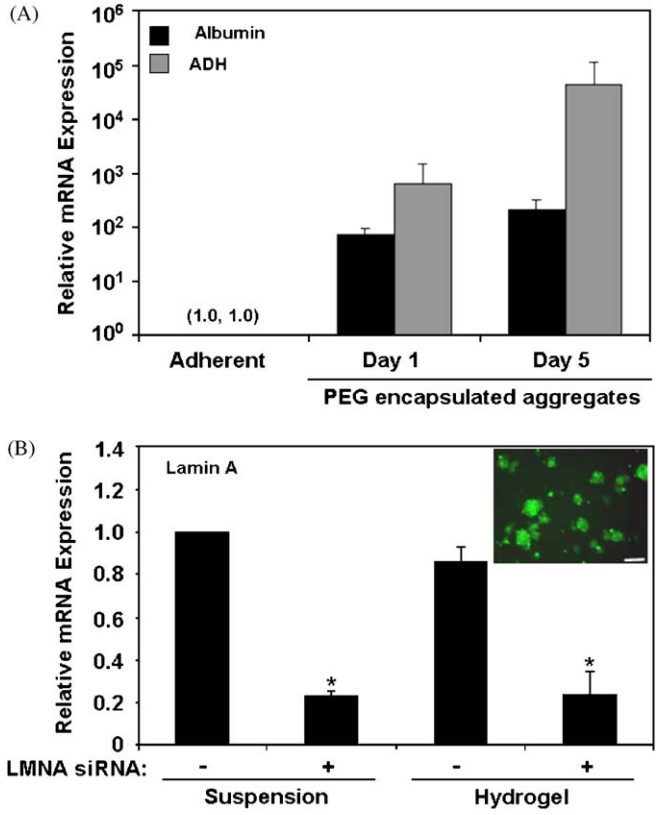

Fig. 2. Analysis of BMEL cell differentiation and gene silencing within PEG hydrogels. (A) Expression of albumin (black bars) and alcohol dehydrogenase (ADH, grey bars) mRNA was determined by real-time quantitative RT-PCR at days 1 and 5 following encapsulation of aggregated BMEL cells in 10% 3.4 kDa PEG hydrogels. Expression for each gene is displayed relative to basal expression exhibited by adherent BMEL cells prior to aggregation. The housekeeping gene, HPRT, was utilized as a normalization control and data are presented as the mean ± SD ($n = 3$). (B) BMEL cells were transfected with fluorescein-labeled lamin A (LMNA) siRNA and then aggregated and encapsulated within 10% 3.4 kDa PEG hydrogels. Fluorescence microscopy illustrates the transfection of encapsulated BMEL cell aggregates (inset, scale bar: 100 μm). LMNA expression was determined by real-time quantitative RT-PCR for suspension or encapsulated aggregates 2 days following transfection with LMNA siRNA (+) or liposome reagent only (−). Expression is shown relative to the expression of HPRT. Data are mean ± SD ($n = 3$). The (*) indicates statistical significance relative to the respective liposome reagent only (−) control, $p < 0.05$ (Student's t-test).

BMEL gene expression within PEG hydrogels, thereby providing important measures of differentiation and gene silencing.

3.3. Survival of PEG hydrogel encapsulated primary hepatocytes

We also extended our analysis of hepatocellular function within PEG hydrogels to primary hepatocytes, a population for which survival and function is recognized to be highly dependent on microenvironmental factors. The majority of primary hepatocytes (75.5 ± 0.03%) were viable within 1 h of encapsulation (Fig. 3A). This partial reduction in the initial viability of primary hepatocytes relative to BMEL cells is likely due to both a modest decrease in the viability of the primary hepatocytes following isolation and perhaps a slight increase in the sensitivity to the encapsulation procedure. Yet, similar to BMEL cells primary hepatocyte viability decreased most substantially following hydrogel culture, with zero viable cells detectable by 1 day post-encapsulation (Fig. 3B). Cell survival measured in parallel by MTT metabolism confirmed this rapid decline in hepatocyte viability (Fig. 3C). In 2D configurations, co-culture of hepatocytes with non-parenchymal cells, including 3T3 fibroblasts, has been shown to improve hepatocyte survival and function [40]. In order to evaluate the effect of fibroblasts on hepatocyte survival within 3D PEG hydrogels, 3T3 fibroblasts were encapsulated with hepatocytes following a stabilization period in standard 2D co-culture, and urea synthesis was measured at multiple time points. Urea synthesis is a component of the ammonia detoxification pathway and is a hepatocyte specific function [46]. In correlation with the viability measures (Figs. 3A–C), hepatocytes encapsulated without fibroblasts displayed a profound and rapid decrease in urea synthesis (Fig. 3D). However, hepatocytes pre-cultured and encapsulated with fibroblasts displayed improved urea synthesis within the hydrogel to a level approximately 40–50% of that exhibited by adherent hepatocytes within the first 24 h following isolation (Fig. 3D). These data demonstrate that non-parenchymal cells are capable of enhancing hepatocyte function within PEG hydrogels. In addition, due to its low molecular weight (~60 Da), the detection of urea synthesis from hydrogel cultures is not limited by the properties of the hydrogel network, and thereby represents a hepatocyte specific function which can be reliably measured in various hydrogel configurations.

3.4. Analysis of primary hepatocyte function within PEG hydrogels

Albumin production and secretion is a critical mature hepatocyte process, which in addition to serving as a marker of hepatocyte differentiation of BMEL cells, is also widely employed as a surrogate measure of overall hepatocyte function. Unlike the detection of synthesized urea, the diffusion of albumin (~65 kDa) from hydrogels can be limited since its size is in the range of the mesh size of commonly utilized hydrogel networks. Previously, it has been demonstrated that both PEG molecular weight and concentration influence mesh size and the diffusion coefficient of biological factors [47]. As a result, we compared the release kinetics of purified albumin from 10% 3.4 kDa PEG hydrogels to hydrogels formed from three different concentrations of a PEG precursor with an increased chain length, 20 kDa (Fig. 4A). Although 20% 20 kDa and 15% 20 kDa gels displayed similar albumin release to the 10% 3.4 kDa gels, 10% 20 kDa hydrogels exhibited significantly increased cumulative albumin release, measured by albumin ELISA, with 74.8 ± 0.08% of

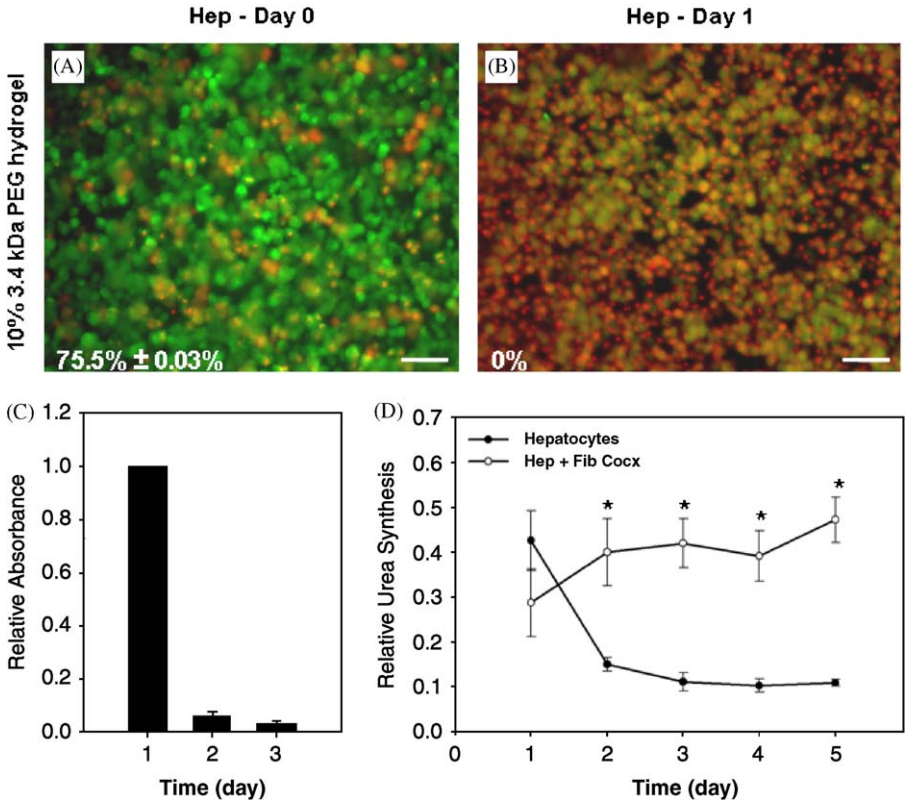

Fig. 3. Co-culture improves primary hepatocyte survival within PEG hydrogels. (A, B) Viability of primary hepatocytes encapsulated in 10% 3.4 kDa PEG hydrogels was evaluated on day 0 (A) and day 1 (B). Fluorescent labeling distinguished viable (green) from nonviable (red) cells. The percentage of viable cells (mean ± SD, $n = 4$) at each time point is indicated. Scale bars: 100 μm. (C) Encapsulated hepatocyte survival was quantitatively assessed using the MTT assay. Absorbance measures are normalized to day 0 values, and data are mean ± SD ($n = 3$). (D) Urea synthesis was quantified for primary hepatocytes encapsulated alone (filled circles), or primary hepatocytes encapsulated with fibroblasts following 2D stabilization (open circles) in 10% 3.4 kDa PEG hydrogels. Values are expressed relative to the urea synthesis of adherent hepatocytes assayed at day 1 of culture to control for animal-to-animal variability. Data are mean ± SD ($n = 3$) and the (*) indicates statistical significance relative to hepatocytes encapsulated alone at the respective time points (Student's *t*-test).

total encapsulated albumin being released from 10% 20 kDa gels within 17 h of gelation (Fig. 4A). These data suggest that hepatocyte culture within 10% 20 kDa hydrogels would improve the release of albumin from the network, thereby enabling the bulk detection of albumin secretion, and therefore, the assessment of another important hepatocyte function.

PEG hydrogels, due to their resistance to non-specific protein adsorption, are generally non-adhesive and do not support cell attachment [12]. Incorporation of adhesive peptides into hydrogel networks has been shown to enhance adhesion and modulate function for a wide range of cell types [48]. Consequently, we investigated the influence of the adhesive peptide, RGDS, on hepatocyte function in the PEG hydrogel system. In order to accurately assess both albumin secretion and urea synthesis from the culture supernatant, 20 kDa PEG-DA was utilized in these experiments. In particular, hepatocyte/fibroblast co-cultures were encapsulated within 10% 20 kDa PEG hydrogels containing PEG alone, or alternatively, PEG plus covalently tethered RGDS or the non-adhesive control peptide, RGES. The presence of the RGDS peptide enhanced hepatocyte function, as albumin secretion was significantly increased upon the incorporation of RGDS relative to RGES at multiple time points, including up to 13 days following encapsulation (Fig. 4B). In independent experiments, substantial albumin secretion has also been detected from encapsulated co-cultures containing RGDS as late as 20 days post-encapsulation (data not shown). Furthermore, there was no significant difference between the PEG only and PEG + RGES conditions (Fig. 4B), implying that the presence of the peptides did not influence hepatocyte function in a non-specific manner. Notably, consistent with albumin secretion, urea synthesis was significantly increased for co-cultures encapsulated in hydrogels containing RGDS (Fig. 4C). Collectively, these data suggest that integrin ligation mediated by the presence of the adhesive peptide RGDS promotes the long-term maintenance of hepatocyte function within PEG hydrogels.

3.5. Imaging of hepatocyte functions within PEG hydrogels

A thorough assessment of hepatocyte processes within the 3D hydrogel platform is predicated upon not only the acquisition of bulk measurements of hepatocyte function

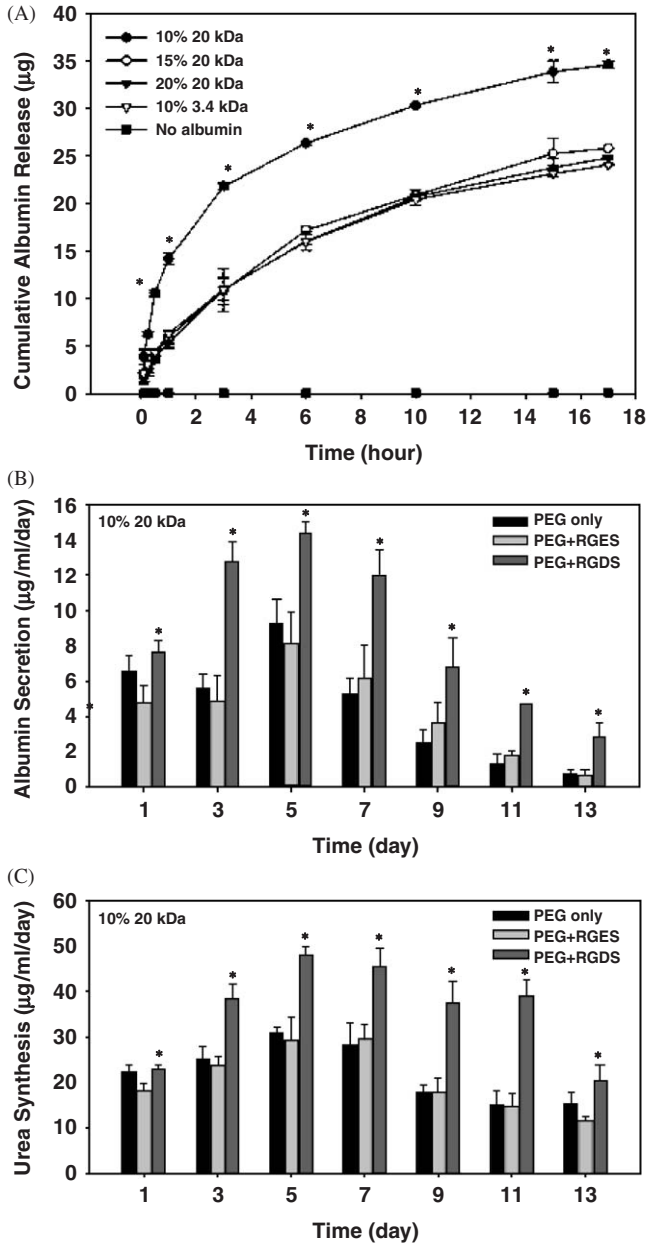

Fig. 4. Hydrogel properties influence release of albumin and long-term hepatocyte function. (A) 40 μg of purified albumin was encapsulated within various hydrogel configurations and the cumulative release was determined by ELISA. Hydrogels without encapsulated albumin (black squares) were used as negative controls. Data are mean ± SD ($n = 4$) and a representative experiment is shown. The (*) indicates statistical significance of 10% 20 kDa hydrogels compared to all other conditions at the specified time points (One-way ANOVA, Tukey post-hoc test). (B, C) Hepatocytes/fibroblast co-cultures were encapsulated in 10% 20 kDa PEG hydrogels containing PEG alone (black bars), PEG + RGES (light grey bars), or PEG + RGDS (dark grey bars) and albumin secretion (B) and urea synthesis (C) was measured at multiple time points. Data are mean ± SD ($n = 3$) and a representative experiment is shown. The (*) indicates statistical difference between PEG + RGDS and PEG + RGES conditions (One-way ANOVA, Tukey post-hoc test).

such as albumin secretion and urea synthesis, but also in situ assays, which provide localized measurements of function at the cellular scale. Similar to native tissues, immunostaining is an important tool for examining protein expression within hydrogel networks. However, the relatively small mesh size of synthetic PEG hydrogels [47], including 10% 20 kDa PEG hydrogels, can limit the effectiveness of antibody-based staining techniques. Sectioning of the hydrogel is consequently required to facilitate efficient antibody labeling; yet the success of any particular sectioning approach is determined by inherent properties of the hydrogel, such as gel stiffness [49]. The sectioning and staining scheme that we optimized for cells encapsulated within 10% 20 kDa PEG hydrogels is outlined in Fig. 5A. Exploiting a paraffin embedding procedure we were able to obtain 10 μm-thick sections, which were subsequently deparaffinized in solution, antibody stained for intracellular albumin, wet mounted, and visualized using conventional fluorescence microscopy (Figs. 5B and C). Utilizing this method, albumin positive hepatocytes are clearly visible within the section, and comparison to the phase contrast image demonstrates that the staining is cell specific (Figs. 5B and C). In addition, hepatocytes are distinguishable from co-encapsulated fibroblasts, which are albumin negative and only label with the Hoechst nuclear stain (Fig. 5C). In particular, the ability to detect intracellular albumin can serve as a tool to identify hepatocytes in the context of a mixed culture, and also permits the assessment of variations in albumin production throughout the network.

Another hepatocyte function which can be evaluated through imaging is glycogen storage. The periodic acid-Schiff (PAS) staining method is a widely utilized histological technique for detecting glycogen within various tissues [50]. In tissue sections treated with the PAS stain, the presence of glycogen, or other highly abundant carbohydrate molecules, is indicated by a purple-magenta coloration. We adapted the conventional PAS staining method to examine glycogen storage of encapsulated hepatocytes in a PEG hydrogel system. Importantly, the chemical components of the PAS protocol diffuse readily into the hydrogel due to their low molecular weight, thereby allowing for the examination of glycogen storage within intact hydrogel networks of assorted configurations, including 3.4 kDa PEG hydrogels, without sectioning. Glycogen staining for hepatocyte/fibroblast co-cultures encapsulated within 10% 3.4 kDa PEG hydrogels containing RGDS was performed at day 4 and day 6 following encapsulation (Figs. 5D and E). Glycogen positive hepatocytes exhibit a dark purple-magenta color, whereas fibroblasts show a light, slightly pink coloration (Figs. 5D and E). Interestingly, at day 6 following encapsulation, some fibroblasts exhibited a spread morphology with spindle-like projections (Fig. 5E). Accordingly, these fibroblasts demonstrate minimal PAS staining, although adjacent hepatocyte clusters display strong coloration indicative of glycogen retention (Fig. 5E). Analogous to intracellular albumin, glycogen labeling through PAS staining can not only provide a means for distinguishing

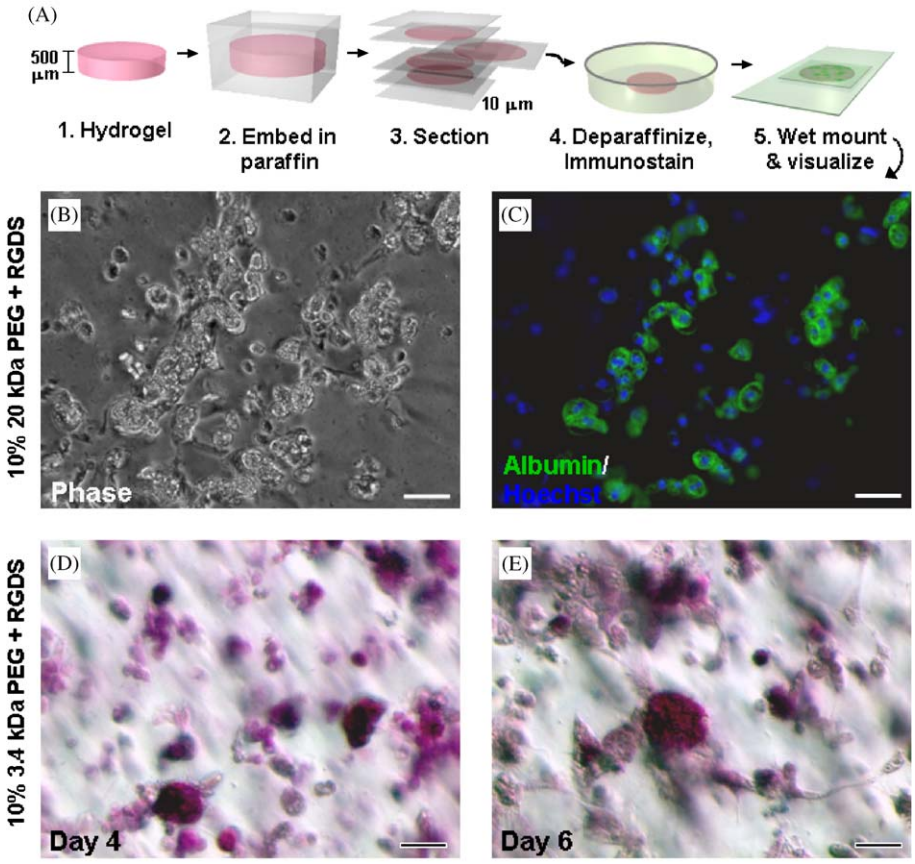

Fig. 5. Localization of encapsulated hepatocyte functions. (A) Diagram of sectioning and staining method optimized for 10% 20 kDa hydrogels. (B, C) 10% 20 kDa PEG hydrogels + RGDS containing encapsulated hepatocyte/fibroblast co-cultures were sectioned (10 μm thick) and stained for intracellular albumin (green) and nuclei were labeled with Hoechst dye (blue). A phase contrast (B) and fluorescence (C) micrograph for a representative field is shown. Scale bars: 25 μm. (D, E) Intact, unsectioned 250 μm thick 10% 3.4 kDa PEG hydrogels + RGDS containing encapsulated hepatocyte/fibroblast co-cultures were stained for glycogen (purple-magenta) with the PAS method on day 4 (D) and day 6 (E) of culture. Scale bars: 25 μm.

hepatocytes from non-parenchymal cells, but also represents another important in situ measurement of encapsulated hepatocyte function.

3.6. Patterning of hepatocellular hydrogel constructs

The photopolymerization property of acrylate-based PEG hydrogels enables the adaptation of photolithographic techniques to generate patterned hydrogel networks [42]. In this process, patterned masks printed on transparencies act to localize the UV exposure of the pre-polymer solution, and thus, dictate the structure of the resultant hydrogel. Utilizing the photopatterning procedure illustrated in Fig. 6A, replicate hydrogel constructs containing BMEL cells were formed. Bright field images (Figs. 6B and D) show the structure of these units, and calcein AM/ethidium homodimer (live/dead) labeling demonstrates the localization and high viability (1 h post-encapsulation) of the encapsulated BMEL cells (Figs. 6C and E) under patterning conditions. In addition, both 500 μm (Figs. 6B and C) and 1 mm (Figs. 6D and E) diameter structures were generated, illustrating the geometric flexibility of this approach.

Photopatterning of hydrogel structures can also be utilized to control cell organization. To demonstrate the capacity to generate hepatocellular hydrogel constructs with defined cellular configurations, we photopatterned PEG hydrogels containing primary hepatocytes and 3T3 fibroblasts. Initially, primary hepatocytes were encapsulated within 500 μm or 1 mm diameter structures as shown for the BMEL cells in Figs. 6B–E. Subsequently, as diagrammed in Fig. 6F, a pre-polymer suspension containing fibroblasts was added and the entire structure was exposed to UV light. The resulting hydrogel network consisted of 3D hepatocyte 'islands' surrounded by regions containing encapsulated fibroblasts. The defined cellular arrangement was demonstrated by glycogen staining 1 h after polymerization, with the hepatocyte islands exhibiting the typical purple-magenta coloration (Figs. 6G and H). Further control of cell orientation within these patterned domains was achieved utilizing dielectrophoretic patterning techniques (Fig. 6I) [43,44], illustrating the ability to manipulate hepatocyte and fibroblast organization at the cellular level (Figs. 6J and K). Additionally, in the dielectrophoretic patterning platform, hepatocytes and fibroblasts are maintained in the bottom plane of the hydrogel, enhancing the capacity to

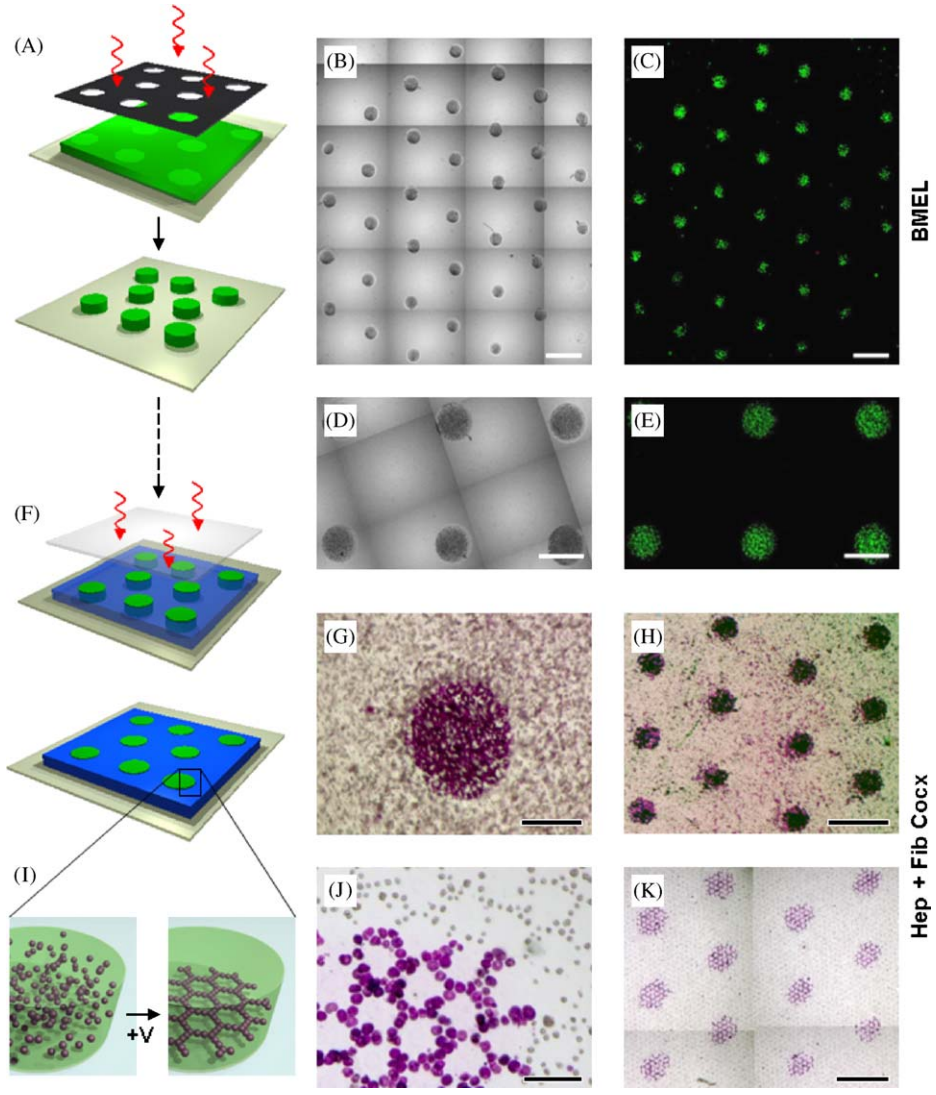

Fig. 6. Hepatocellular hydrogel constructs with highly defined architecture and cellular organization. (A) Schematic of photopatterning technique utilized to generate an array of hydrogel units. (B–E) Bright field images demonstrate the formation of replicate ~500 μm (B) or ~1 mm (D) diameter hydrogel structures containing encapsulated BMEL cells. (C, E) Live/dead labeling performed 1 h following polymerization identifies viable (green) and nonviable (red) BMEL cells within these respective structures. Scale bars: 1 mm. (F) Diagram illustrating secondary polymerization of a surrounding hydrogel region within the same thickness plane. (G, H) Encapsulated hepatocytes were initially patterned in ~1 mm (G) or ~500 μm (H) diameter islands followed by the polymerization of a surrounding hydrogel network containing encapsulated fibroblasts. Hepatocyte specific glycogen staining (1 h post-polymerization, purple-magenta) demonstrates the localization of these hepatocyte domains. Scale bars: 500 μm (G), 1 mm (H). (I) Schematic of dielectrophoretic patterning method. (J, K) Hepatocytes organized via electropatterning were entrapped in islands by photopatterning and then surrounded by electropatterned encapsulated fibroblasts. Glycogen staining (1 h post polymerization, purple-magenta) was performed on these dual patterned constructs. Scale bars: 100 μm (J), 1 mm (K).

visualize and track individual cells. Taken together, these examples highlight the ability of photopatterning and dielectrophoretic patterning techniques to control the overall architecture of hepatocellular PEG hydrogel constructs.

4. Discussion

In this study we employed a spectrum of cellular and molecular biology techniques to examine the survival and function of BMEL cells and primary hepatocytes within PEG hydrogels. Previously, we and others have shown that hydrogel polymerization parameters such as photoinitiator type and concentration, UV intensity, and duration of UV exposure influence encapsulated cell viability [42,45]. Utilizing conditions recognized to induce minimal toxicity in a wide range of cell types, we were able to generate BMEL cell and primary hepatocyte hydrogel constructs which exhibited high initial viability (Figs. 1 and 3). However, both BMEL cells and hepatocytes subsequently exhibited marked losses in viability upon encapsulation alone as monodispersed populations (Figs. 1 and 3). Cell–cell interactions have been previously demonstrated to play a key role in the inhibition of apoptosis in many

systems [51–53]. Of particular relevance is the observation that BMEL cells cultured in non-adhesive plates readily survive as spheroidal aggregates in suspension, a configuration which induced the upregulation of hepatocyte markers [35]. Consistent with these findings, pre-aggregation of BMEL cells significantly improved survival following hydrogel encapsulation (Fig. 1). An analogous increase in BMEL cell viability for aggregates versus dispersed cells was observed in hydrogel networks formed from 20 kDa PEG molecules. Specifically, BMEL cell aggregates in 20 kDa PEG hydrogels exhibited on average a 2.95-fold increase in viability on day 3 relative to dispersed cells (data not shown) similar to the 2.72-fold increase within 3.4 kDa gels (Fig. 1E), suggesting that hydrogel parameters dictated by PEG chain length, such as mesh size, do not directly influence the viability of encapsulated BMEL cells. Taken together, these data underscore the importance of homotypic cell–cell interactions in the maintenance of BMEL cell survival within the inert PEG hydrogel environment.

Quantitative gene expression analysis for encapsulated cells illustrated that BMEL cell differentiation towards the hepatocyte lineage can proceed efficiently within the framework of the PEG hydrogel (Fig. 2). We also demonstrated the ability to identify transfected cells and evaluate siRNA-mediated gene silencing of BMEL cells within the gel network (Fig. 2). Transfection of pre-encapsulated cells poses another option for these types of studies, although potential diffusive limitations of standard carrier reagents will likely necessitate significant optimization of the delivery of siRNA complexes. Overall, the compatibility of BMEL cell differentiation with hydrogel culture coupled with the capacity to assess and modulate encapsulated cell gene expression represents the foundation for the detailed analysis of BMEL cell processes in a 3D context. For example, the PEG hydrogel system enables the incorporation of distinct biologically active elements, and thus, the potential identification of elements that influence BMEL cell proliferation, survival of dispersed cells, and differentiation efficiency. PEG hydrogels have been previously utilized as 3D platforms for the differentiation of adipocyte precursor cells [54], adult mesenchymal stem cells [29,31,33,55], and embryonic stem cells [56], yet the differentiation of liver progenitor cells in this system has not been investigated. Importantly, BMEL cells, as their designation implies, are bipotential, and can differentiate into hepatocytes as well as bile duct epithelial cells [35,36]. In vitro culture of BMEL cells in Matrigel has been shown to induce the upregulation of bile duct markers, such as GGT IV, HNF6, and Thy-1 [35]. Incorporation of bioactive factors into the PEG hydrogel system that mimic components of Matrigel or various in vivo environmental stimuli could provide important information regarding the mechanisms controlling BMEL cell fate specification.

We also examined factors that affect the stability of primary hepatocyte function in PEG hydrogels. Although many diverse approaches have been investigated for 3D culture of hepatocytes including the deposition of hepatocyte-containing gelatin structures [57], culture within an array of channels [58,59], microencapsulation of hepatocyte spheroids [6,60], and seeding of pre-formed scaffolds [61], the culture of primary hepatocytes within the PEG hydrogel platform has been considerably less explored. Similar to the impact on BMEL cells, cell–cell interactions have been implicated in the maintenance of hepatocyte survival in culture [40,62–65]. For instance, 2D co-culture of hepatocytes with 3T3 fibroblasts represents a well characterized and robust platform for the in vitro stabilization of hepatocytes [40]. In this report, we demonstrate that fibroblast co-culture can influence hepatocyte function in a 3D context, as fibroblasts promoted the maintenance of primary hepatocyte function within PEG hydrogels (Fig. 3). In these randomly organized co-cultures, long-term hepatocyte function is likely maintained through the combinatorial influence of both paracrine and cell contact-mediated signals provided by the fibroblasts. Further elucidation of the mechanisms of this co-culture effect in 3D is an aim of future studies and would likely benefit from patterning technologies illustrated here and discussed in more detail below.

In addition to the presence of fibroblasts, conjugation of the adhesive peptide, RGDS, to the hydrogel network further improved functionality of hepatocytes within hydrogels (Fig. 4). Tethered RGD moieties have been previously demonstrated to mediate fibroblast [66–69], endothelial cell [70–72], and smooth muscle cell adhesion and migration [24,73,74]. RGD presenting hydrogels can also support osteoblast, myoblast, and mesenchymal stem cell differentiation [26,30,75–77], as well as influence protein production of SV40 immortalized hepatocytes [78]. The long-term enhancement of albumin secretion and urea synthesis within RGDS containing hydrogels described here highlights the importance of RGD-mediated adhesive interactions in overall primary hepatocyte stability in 3D. Interestingly, the orientation of extracellular matrix presentation (2D versus 3D) can be an important determinant of cellular responses. For example, culture of hepatocytes in collagen gel as opposed to monolayer can dictate changes in the cytoskeleton, integrin distribution, and gene expression [65,79–81]. Furthermore, the degree of cross-talk between signaling pathways can be influenced by culture dimensions. Such an effect has been noted for mammary epithelial cells, in which interactions between $\beta 1$ integrin and EGF receptor have been identified in 3D, but not 2D cultures [82]. Additional analysis of hepatocyte functions in the presence of peptide-conjugated PEG hydrogel substrates will provide insight regarding the mechanisms of hepatocyte stabilization and the specific effects of dimensionality in hepatocyte functions.

The versatility of the PEG system allows for the independent optimization of parameters affecting multiple aspects of cellular function. In previous studies, numerous PEG hydrogel formulations, including PEG chain lengths ranging from 0.5 to 20 kDa, weight percentages ranging

from 10% to 30%, and single-arm and multi-arm PEG molecules have been utilized for the encapsulation of a wide range of cell types [83]. Here, we demonstrate that hepatocyte culture within 10% 20 kDa PEG hydrogels enables the efficient release of albumin (Fig. 4), and thus, the 20 kDa chain length was utilized in experiments in which secreted albumin from encapsulated hepatocytes was assessed. Of note, adequate exchange of relatively large macromolecules, such as albumin, represents an important parameter for the development of implantable liver constructs. Moreover, as illustrated by the effect of RGDS on encapsulated hepatocyte function, further improvement of functionality could potentially be achieved within these constructs by the integration of additional acellular factors such as recombinant cellular ligands or adhesive peptides that bind other integrin receptors. Hydrolytic or protease-sensitive domains can also be incorporated into PEG hydrogel networks [23,54,70,84–86], which would allow for the degradation of the hepatocellular constructs upon implantation.

Imaging of cellular functions within PEG hydrogels poses a unique challenge, most notably due to the diffusive limitations imposed by the relatively small mesh size of the networks. As a result, histological assays based on small, readily diffusible components are important tools for the assessment of cellular function within intact hydrogel networks. For example, Alcian Blue dye labeling has been used previously to localize and quantify the deposition of sulfated glycosaminoglycans in the PEG hydrogel system [14,44,87]. Here we demonstrate hepatocyte-specific glycogen staining within intact PEG hydrogels (Fig. 5). Glycogen storage is an important hepatocyte process that has been shown to be influenced by cell–cell communication [88,89]. Consequently, in addition to its applicability as a tool to specifically identify hepatocytes, examination of glycogen retention within PEG hydrogels would supply information regarding the effects of 3D culture configurations on hepatocyte metabolism. In a similar fashion, immunostaining of hydrogel networks can serve to identify cells and concurrently provide measures of localized cellular functions. Yet, unlike small molecule-based histological techniques, sectioning of the hydrogel structure is required to enable sufficient antibody labeling. A multitude of histological techniques have been explored for the processing of biomaterial scaffolds, including vibratome sectioning, cryosectioning, paraffin embedding, and the use of hard plastic resins [24,28,29,49,56,90–92]. Although vibratome and cryostat sectioning have been used extensively for lower molecular weight PEG hydrogels [24,28,31,73], we were unable to generate adequate sections from 10% 20 kDa PEG hydrogels using these techniques due to limitations imposed by the highly elastic nature of these gels (unpublished observations) [93]. However, utilizing a paraffin embedding procedure described in Section 2 and outlined in Fig. 5, we were able to obtain intact sections which were used to assay for intracellular albumin expression. This sectioning and staining technique could be generally utilized for analyzing the expression of a broad spectrum of proteins for hydrogel encapsulated hepatic cells.

Finally, photoactive hydrogel systems for cell encapsulation offer the unique ability to apply photolithographic techniques towards the formation of patterned structures. Other commonly utilized techniques for patterning cellular structures include microfluidics and micromolding [94–97]. The major advantages of photolithography-based techniques for patterning of hydrogel structures are its simplicity and flexibility. Photopatterning technology has been utilized to surface pattern biological factors [98], produce hydrogel structures with a range of sizes and shapes [99,100], as well as build multilayer cellular constructs [42]. Utilizing photopatterning techniques we demonstrated in this study the generation of an array of replicate BMEL cell containing hydrogel units (Fig. 6). Such an array could serve as a platform for the parallel investigation of factors influencing BMEL cell functions in 3D hydrogel culture. For example, integration with other technologies, such as microfluidics, would allow for the high-throughput examination of the influence of soluble stimuli, and incorporation of additional masking and polymerization steps would enable the development of encapsulated cellular arrays with distinct spatially defined hydrogel chemistries. In addition to the formation of replicate structures for parallel analysis, photopatterning techniques can also facilitate the construction of more complex multicellular hydrogel structures [42,43]. We illustrate here the formation of co-culture hydrogel networks with a highly defined architecture (Fig. 6). In particular, using photopatterning techniques the localization and interface of hepatocyte and fibroblast regions within the hydrogel structures was controlled. Moreover, employing a dielectrophoretic patterning method recently utilized to investigate chondrocyte cell–cell interactions in 3D [44], we generated hydrogel structures with hepatocyte and fibroblast organization defined at the cellular scale. Notably, surface chemistry-mediated micropatterning of hepatoctye/fibroblast co-cultures has been shown to play an important role in hepatocyte function in 2D cultures [40]. Thus, patterning of hydrogel networks allows for the extension of these studies of hepatocyte and fibroblast communication to a 3D context including the determination of the relative involvement of key paracrine and cell contact-mediated signals. Furthermore, the multiscale regulation of cell positioning within hydrogel platforms represents an important step towards the development of hydrogel constructs exhibiting the range of organizational elements crucial for hepatocellular function.

5. Conclusions

In this study we utilized an array of cellular and molecular biology techniques to examine factors influencing the survival and function of hepatic cells within the PEG hydrogel platform. Assays for encapsulated cell

viability and hepatocyte-specific function demonstrated the importance of cell–cell and cell–matrix interactions in BMEL cell and primary hepatocyte survival in hydrogel culture. Additionally, quantitative gene expression analysis of encapsulated cells illustrated the compatibility of BMEL cell differentiation with hydrogel culture and the capacity to regulate gene expression through RNA interference. We further illustrated imaging tools for the direct visualization of hepatic cell functions within PEG hydrogels and the capacity to control cellular organization and hydrogel structure through the use of photopatterning and dielectrophoretic patterning methods. Collectively, these techniques and the insight regarding BMEL cell and hepatocyte function in PEG hydrogels provided in these studies present a versatile platform for studying liver biology and development and establish a foundation for the further development of highly functional hydrogel-based implantable liver systems.

Acknowledgements

We gratefully acknowledge M. Weiss and H. Strick-Marchand for providing the BMEL 9A1 cell line and K. Hudson and M. Akiyama for hepatocyte isolation. Funding was provided by NIH (S.N.B., G.H.U.), NSF (S.N.B., A.A.C.), the Whitaker Foundation (D.R.A.), the David and Lucille Packard Foundation, and NASA.

References

[1] Allen JW, Bhatia SN. Engineering liver therapies for the future. Tissue Eng 2002;8:725–37.
[2] Allen JW, Bhatia SN. Improving the next generation of bioartificial liver devices. Semin Cell Dev Biol 2002;13:447–54.
[3] Balis UJ, Behnia K, Dwarakanath B, Bhatia SN, Sullivan SJ, Yarmush ML, et al. Oxygen consumption characteristics of porcine hepatocytes. Metab Eng 1999;1:49–62.
[4] Demetriou AA, Whiting JF, Feldman D, Levenson SM, Chowdhury NR, Moscioni AD, et al. Replacement of liver function in rats by transplantation of microcarrier-attached hepatocytes. Science 1986;233:1190–2.
[5] Demetriou AA, Levenson SM, Novikoff PM, Novikoff AB, Chowdhury NR, Whiting J, et al. Survival, organization, and function of microcarrier-attached hepatocytes transplanted in rats. Proc Natl Acad Sci USA 1986;83:7475–9.
[6] Hamazaki K, Doi Y, Koide N. Microencapsulated multicellular spheroid of rat hepatocytes transplanted intraperitoneally after 90% hepatectomy. Hepatogastroenterology 2002;49:1514–6.
[7] Dixit V, Arthur M, Reinhardt R, Gitnick G. Improved function of microencapsulated hepatocytes in a hybrid bioartificial liver support system. Artif Organs 1992;16:336–41.
[8] Kaihara S, Borenstein J, Koka R, Lalan S, Ochoa ER, Ravens M, et al. Silicon micromachining to tissue engineer branched vascular channels for liver fabrication. Tissue Eng 2000;6:105–17.
[9] Mooney DJ, Sano K, Kaufmann PM, Majahod K, Schloo B, Vacanti JP, et al. Long-term engraftment of hepatocytes transplanted on biodegradable polymer sponges. J Biomed Mater Res 1997;37:413–20.
[10] Vacanti JP, Morse MA, Saltzman WM, Domb AJ, Perez-Atayde A, Langer R. Selective cell transplantation using bioabsorbable artificial polymers as matrices. J Pediatr Surg 1988;23:3–9.
[11] Dvir-Ginzberg M, Gamlieli-Bonshtein I, Agbaria R, Cohen S. Liver tissue engineering within alginate scaffolds: effects of cell-seeding density on hepatocyte viability, morphology, and function. Tissue Eng 2003;9:757–66.
[12] Peppas NA, Bures P, Leobandung W, Ichikawa H. Hydrogels in pharmaceutical formulations. Eur J Pharm Biopharm 2000;50:27–46.
[13] Lutolf MP, Hubbell JA. Synthetic biomaterials as instructive extracellular microenvironments for morphogenesis in tissue engineering. Nat Biotechnol 2005;23:47–55.
[14] Riley SL, Dutt S, De La Torre R, Chen AC, Sah RL, Ratcliffe A. Formulation of PEG-based hydrogels affects tissue-engineered cartilage construct characteristics. J Mater Sci Mater Med 2001;12:983–90.
[15] Bryant SJ, Anseth KS, Lee DA, Bader DL. Crosslinking density influences the morphology of chondrocytes photoencapsulated in PEG hydrogels during the application of compressive strain. J Orthop Res 2004;22:1143–9.
[16] Bryant SJ, Bender RJ, Durand KL, Anseth KS. Encapsulating chondrocytes in degrading PEG hydrogels with high modulus: engineering gel structural changes to facilitate cartilaginous tissue production. Biotechnol Bioeng 2004;86:747–55.
[17] Bryant SJ, Chowdhury TT, Lee DA, Bader DL, Anseth KS. Crosslinking density influences chondrocyte metabolism in dynamically loaded photocrosslinked poly(ethylene glycol) hydrogels. Ann Biomed Eng 2004;32:407–17.
[18] Park Y, Lutolf MP, Hubbell JA, Hunziker EB, Wong M. Bovine primary chondrocyte culture in synthetic matrix metalloproteinase-sensitive poly(ethylene glycol)-based hydrogels as a scaffold for cartilage repair. Tissue Eng 2004;10:515–22.
[19] Martens PJ, Bryant SJ, Anseth KS. Tailoring the degradation of hydrogels formed from multivinyl poly(ethylene glycol) and poly(vinyl alcohol) macromers for cartilage tissue engineering. Biomacromolecules 2003;4:283–92.
[20] Lee SH, Miller JS, Moon JJ, West JL. Proteolytically degradable hydrogels with a fluorogenic substrate for studies of cellular proteolytic activity and migration. Biotechnol Prog 2005;21:1736–41.
[21] Gobin AS, West JL. Effects of epidermal growth factor on fibroblast migration through biomimetic hydrogels. Biotechnol Prog 2003;19:1781–5.
[22] Raeber GP, Lutolf MP, Hubbell JA. Molecularly engineered PEG hydrogels: a novel model system for proteolytically mediated cell migration. Biophys J 2005;89:1374–88.
[23] Lutolf MP, Lauer-Fields JL, Schmoekel HG, Metters AT, Weber FE, Fields GB, et al. Synthetic matrix metalloproteinase-sensitive hydrogels for the conduction of tissue regeneration: engineering cell-invasion characteristics. Proc Natl Acad Sci USA 2003;100:5413–8.
[24] Mann BK, Gobin AS, Tsai AT, Schmedlen RH, West JL. Smooth muscle cell growth in photopolymerized hydrogels with cell adhesive and proteolytically degradable domains: synthetic ECM analogs for tissue engineering. Biomaterials 2001;22:3045–51.
[25] Mann BK, Schmedlen RH, West JL. Tethered-TGF-beta increases extracellular matrix production of vascular smooth muscle cells. Biomaterials 2001;22:439–44.
[26] Burdick JA, Anseth KS. Photoencapsulation of osteoblasts in injectable RGD-modified PEG hydrogels for bone tissue engineering. Biomaterials 2002;23:4315–23.
[27] Burdick JA, Mason MN, Hinman AD, Thorne K, Anseth KS. Delivery of osteoinductive growth factors from degradable PEG hydrogels influences osteoblast differentiation and mineralization. J Control Release 2002;83:53–63.
[28] Mahoney MJ, Anseth KS. Three-dimensional growth and function of neural tissue in degradable polyethylene glycol hydrogels. Biomaterials 2006;27:2265–74.
[29] Nuttelman CR, Tripodi MC, Anseth KS. In vitro osteogenic differentiation of human mesenchymal stem cells photoencapsulated in PEG hydrogels. J Biomed Mater Res 2004;68A:773–82.

[30] Nuttelman CR, Tripodi MC, Anseth KS. Synthetic hydrogel niches that promote hMSC viability. Matrix Biol 2005;24:208–18.
[31] Nuttelman CR, Tripodi MC, Anseth KS. Dexamethasone-functionalized gels induce osteogenic differentiation of encapsulated hMSCs. J Biomed Mater Res A 2006;76:183–95.
[32] Wang DA, Williams CG, Li Q, Sharma B, Elisseeff JH. Synthesis and characterization of a novel degradable phosphate-containing hydrogel. Biomaterials 2003;24:3969–80.
[33] Wang DA, Williams CG, Yang F, Cher N, Lee H, Elisseeff JH. Bioresponsive phosphoester hydrogels for bone tissue engineering. Tissue Eng 2005;11:201–13.
[34] Lemaigre F, Zaret KS. Liver development update: new embryo models, cell lineage control, and morphogenesis. Curr Opin Genet Dev 2004;14:582–90.
[35] Strick-Marchand H, Weiss MC. Inducible differentiation and morphogenesis of bipotential liver cell lines from wild-type mouse embryos. Hepatology 2002;36:794–804.
[36] Strick-Marchand H, Morosan S, Charneau P, Kremsdorf D, Weiss MC. Bipotential mouse embryonic liver stem cell lines contribute to liver regeneration and differentiate as bile ducts and hepatocytes. Proc Natl Acad Sci USA 2004;101:8360–5.
[37] Seglen PO. Preparation of isolated rat liver cells. Methods Cell Biol 1976;13:29–83.
[38] Dunn JC, Tompkins RG, Yarmush ML. Long-term in vitro function of adult hepatocytes in a collagen sandwich configuration. Biotechnol Prog 1991;7:237–45.
[39] Rheinwald JG, Green H. Serial cultivation of strains of human epidermal keratinocytes: the formation of keratinizing colonies from single cells. Cell 1975;6:331–43.
[40] Bhatia SN, Balis UJ, Yarmush ML, Toner M. Effect of cell–cell interactions in preservation of cellular phenotype: cocultivation of hepatocytes and nonparenchymal cells. Faseb J 1999;13:1883–900.
[41] Khetani SR, Szulgit G, Del Rio JA, Barlow C, Bhatia SN. Exploring interactions between rat hepatocytes and nonparenchymal cells using gene expression profiling. Hepatology 2004;40:545–54.
[42] Liu VA, Bhatia SN. Three-dimensional photopatterning of hydrogels containing living cells. Biomedical Microdevices 2002;4:257–66.
[43] Albrecht DR, Tsang VL, Sah RL, Bhatia SN. Photo- and electropatterning of hydrogel-encapsulated living cell arrays. Lab Chip 2005;5:111–8.
[44] Albrecht DR, Underhill GH, Wassermann TB, Sah RL, Bhatia SN. Probing the role of multicellular organization in 3D microenvironments. Nat Methods 2006;3:369–75.
[45] Williams CG, Malik AN, Kim TK, Manson PN, Elisseeff JH. Variable cytocompatibility of six cell lines with photoinitiators used for polymerizing hydrogels and cell encapsulation. Biomaterials 2005;26:1211–8.
[46] Zakim D, Boyer TD. Hepatology: a textbook of liver disease. 2nd ed. Philadelphia: Saunders; 1990.
[47] Cruise GM, Scharp DS, Hubbell JA. Characterization of permeability and network structure of interfacially photopolymerized poly(ethylene glycol) diacrylate hydrogels. Biomaterials 1998;19:1287–94.
[48] Hubbell JA. Bioactive biomaterials. Curr Opin Biotechnol 1999;10:123–9.
[49] James R, Jenkins L, Ellis SE, Burg KJL. Histological processing of hydrogel scaffolds for tissue-engineering applications. J Histotechnol 2004;27:133–9.
[50] Lake BD. The histochemical evaluation of the glycogen storage diseases. A review of techniques and their limitations. Histochem J 1970;2:441–50.
[51] Bates RC, Edwards NS, Yates JD. Spheroids and cell survival. Crit Rev Oncol Hematol 2000;36:61–74.
[52] Zahir N, Weaver VM. Death in the third dimension: apoptosis regulation and tissue architecture. Curr Opin Genet Dev 2004;14:71–80.
[53] Grossmann J. Molecular mechanisms of "detachment-induced apoptosis–Anoikis". Apoptosis 2002;7:247–60.
[54] Patel PN, Gobin AS, West JL, Patrick Jr CW. Poly(ethylene glycol) hydrogel system supports preadipocyte viability, adhesion, and proliferation. Tissue Eng 2005;11:1498–505.
[55] Alhadlaq A, Tang M, Mao JJ. Engineered adipose tissue from human mesenchymal stem cells maintains predefined shape and dimension: implications in soft tissue augmentation and reconstruction. Tissue Eng 2005;11:556–66.
[56] Hwang NS, Kim MS, Sampattavanich S, Baek JH, Zhang Z, Elisseeff J. Effects of three-dimensional culture and growth factors on the chondrogenic differentiation of murine embryonic stem cells. Stem Cells 2006;24:284–91.
[57] Wang X, Yan Y, Pan Y, Xiong Z, Liu H, Cheng J, et al. Generation of three-dimensional hepatocyte/gelatin structures with rapid prototyping system. Tissue Eng 2006;12:83–90.
[58] Powers MJ, Domansky K, Kaazempur-Mofrad MR, Kalezi A, Capitano A, Upadhyaya A, et al. A microfabricated array bioreactor for perfused 3D liver culture. Biotechnol Bioeng 2002;78:257–69.
[59] Powers MJ, Janigian DM, Wack KE, Baker CS, Stolz DB, Griffith LG. Functional behavior of primary rat liver cells in a three-dimensional perfused microarray bioreactor. Tissue Eng 2002;8:499–513.
[60] Quek CH, Li J, Sun T, Chan ML, Mao HQ, Gan LM, et al. Photocrosslinkable microcapsules formed by polyelectrolyte copolymer and modified collagen for rat hepatocyte encapsulation. Biomaterials 2004;25:3531–40.
[61] Hammond JS, Beckingham IJ, Shakesheff KM. Scaffolds for liver tissue engineering. Exp Rev Med Dev 2006;3:21–7.
[62] Corlu A, Ilyin G, Cariou S, Lamy I, Loyer P, Guguen-Guillouzo C. The coculture: a system for studying the regulation of liver differentiation/proliferation activity and its control. Cell Biol Toxicol 1997;13:235–42.
[63] Landry J, Bernier D, Ouellet C, Goyette R, Marceau N. Spheroidal aggregate culture of rat liver cells: histotypic reorganization, biomatrix deposition, and maintenance of functional activities. J Cell Biol 1985;101:914–23.
[64] Saito S, Sakagami K, Matsuno T, Tanakaya K, Takaishi Y, Orita K. Long-term survival and proliferation of spheroidal aggregate cultured hepatocytes transplanted into the rat spleen. Transplant Proc 1992;24:1520–1.
[65] Moghe PV, Coger RN, Toner M, Yarmush ML. Cell–cell interactions are essential for maintenance of hepatocyte function in collagen gel but not on matrigel. Biotechnol Bioeng 1997;56:706–11.
[66] Hern DL, Hubbell JA. Incorporation of adhesion peptides into nonadhesive hydrogels useful for tissue resurfacing. J Biomed Mater Res 1998;39:266–76.
[67] VandeVondele S, Voros J, Hubbell JA. RGD-grafted poly-L-lysine-graft-(polyethylene glycol) copolymers block non-specific protein adsorption while promoting cell adhesion. Biotechnol Bioeng 2003;82:784–90.
[68] Mi L, Fischer S, Chung B, Sundelacruz S, Harden JL. Self-assembling protein hydrogels with modular integrin binding domains. Biomacromolecules 2006;7:38–47.
[69] Park YD, Tirelli N, Hubbell JA. Photopolymerized hyaluronic acid-based hydrogels and interpenetrating networks. Biomaterials 2003;24:893–900.
[70] Seliktar D, Zisch AH, Lutolf MP, Wrana JL, Hubbell JA. MMP-2 sensitive, VEGF-bearing bioactive hydrogels for promotion of vascular healing. J Biomed Mater Res 2004;68A:704–16.
[71] Fittkau MH, Zilla P, Bezuidenhout D, Lutolf MP, Human P, Hubbell JA, et al. The selective modulation of endothelial cell mobility on RGD peptide containing surfaces by YIGSR peptides. Biomaterials 2005;26:167–74.
[72] Zisch AH, Lutolf MP, Ehrbar M, Raeber GP, Rizzi SC, Davies N, et al. Cell-demanded release of VEGF from synthetic, biointeractive

cell ingrowth matrices for vascularized tissue growth. Faseb J 2003;17:2260–2.
[73] Mann BK, West JL. Cell adhesion peptides alter smooth muscle cell adhesion, proliferation, migration, and matrix protein synthesis on modified surfaces and in polymer scaffolds. J Biomed Mater Res 2002;60:86–93.
[74] DeLong SA, Moon JJ, West JL. Covalently immobilized gradients of bFGF on hydrogel scaffolds for directed cell migration. Biomaterials 2005;26:3227–34.
[75] Rowley JA, Madlambayan G, Mooney DJ. Alginate hydrogels as synthetic extracellular matrix materials. Biomaterials 1999;20: 45–53.
[76] Alsberg E, Anderson KW, Albeiruti A, Franceschi RT, Mooney DJ. Cell-interactive alginate hydrogels for bone tissue engineering. J Dent Res 2001;80:2025–9.
[77] Behravesh E, Mikos AG. Three-dimensional culture of differentiating marrow stromal osteoblasts in biomimetic poly(propylene fumarate-*co*-ethylene glycol)-based macroporous hydrogels. J Biomed Mater Res A 2003;66:698–706.
[78] Itle LJ, Koh WG, Pishko MV. Hepatocyte viability and protein expression within hydrogel microstructures. Biotechnol Prog 2005;21:926–32.
[79] Moghe PV, et al. Collagen sandwich and Matrigel cultures of rat hepatocytes elicit comparable function but different cell polarity and cytoskeletal organization: Implications for optimal ECM design. Mol Biol Cell 1994;5(suppl.):177A.
[80] Moghe PV, Parashurama N, Ezzell RM, Toner M, Tompkins RG, Yarmush ML. Effect of collagen gel configuration on integrin localization in cultured rat hepatocytes. Mol Biol Cell 1995;6(suppl.):238A.
[81] Moghe PV, Berthiaume F, Ezzell RM, Toner M, Tompkins RG, Yarmush ML. Culture matrix configuration and composition in the maintenance of hepatocyte polarity and function. Biomaterials 1996;17:373–85.
[82] Wang F, Weaver VM, Petersen OW, Larabell CA, Dedhar S, Briand P, et al. Reciprocal interactions between beta1-integrin and epidermal growth factor receptor in three-dimensional basement membrane breast cultures: a different perspective in epithelial biology. Proc Natl Acad Sci USA 1998;95:14821–6.
[83] Nguyen KT, West JL. Photopolymerizable hydrogels for tissue engineering applications. Biomaterials 2002;23:4307–14.
[84] Sawhney AS, Pathak CP, Hubbell JA. Bioerodible hydrogels based on photopolymerized poly(ethylene glycol)-*co*-poly(a-hydroxy acid) diacrylate macromers. Macromolecules 1993;26:581–7.
[85] Davis KA, Burdick JA, Anseth KS. Photoinitiated crosslinked degradable copolymer networks for tissue engineering applications. Biomaterials 2003;24:2485–95.
[86] Anseth KS, Metters AT, Bryant SJ, Martens PJ, Elisseeff JH, Bowman CN. In situ forming degradable networks and their application in tissue engineering and drug delivery. J Control Release 2002;78:199–209.
[87] Farndale RW, Sayers CA, Barrett AJ. A direct spectrophotometric microassay for sulfated glycosaminoglycans in cartilage cultures. Connect Tissue Res 1982;9:247–8.
[88] Siddiqui MU, Benatmane S, Zachayus JL, Plas C. Gap junctional communication and regulation of the glycogenic response to insulin by cell density and glucocorticoids in cultured fetal rat hepatocytes. Hepatology 1999;29:1147–55.
[89] Eugenin EA, Gonzalez H, Saez CG, Saez JC. Gap junctional communication coordinates vasopressin-induced glycogenolysis in rat hepatocytes. Am J Physiol 1998;274:G1109–16.
[90] Webster SS, Jenkins L, Burg KJL. Histological techniques for porous, absorbable, polymeric scaffolds used in tissue engineering. J Histotechnol 2003;26:57–65.
[91] Moore K, MacSween M, Shoichet M. Immobilized concentration gradients of neurotrophic factors guide neurite outgrowth of primary neurons in macroporous scaffolds. Tissue Eng 2006;12: 267–78.
[92] Jun HW, West JL. Endothelialization of microporous YIGSR/PEG-modified polyurethaneurea. Tissue Eng 2005;11:1133–40.
[93] Anseth KS, Bowman CN, Brannon-Peppas L. Mechanical properties of hydrogels and their experimental determination. Biomaterials 1996;17:1647–57.
[94] Tan W, Desai TA. Microfluidic patterning of cellular biopolymer matrices for biomimetic 3D structures. Biomed Microdev 2003;5:235–44.
[95] Tan W, Desai TA. Layer-by-layer microfluidics for biomimetic three-dimensional structures. Biomaterials 2004;25:1355–64.
[96] Suh KY, Seong J, Khademhosseini A, Laibinis PE, Langer R. A simple soft lithographic route to fabrication of poly(ethylene glycol) microstructures for protein and cell patterning. Biomaterials 2004;25:557–63.
[97] Khademhosseini A, Jon S, Suh KY, Tran TNT, Eng G, Yeh J, et al. Direct patterning of protein- and cell-resistant polymeric monolayers and microstructures. Adv Mater 2003;15:1995–2000.
[98] Hahn MS, Taite LJ, Moon JJ, Rowland MC, Ruffino KA, West JL. Photolithographic patterning of polyethylene glycol hydrogels. Biomaterials 2006;27:2519–24.
[99] Revzin A, Russell RJ, Yadavalli VK, Koh WG, Deister C, Hile DD, et al. Fabrication of poly(ethylene glycol) hydrogel microstructures using photolithography. Langmuir 2001;17:5440–7.
[100] Beebe DJ, Moore JS, Bauer JM, Yu Q, Liu RH, Devadoss C, et al. Functional hydrogel structures for autonomous flow control inside microfluidic channels. Nature 2000;404:588–90.